



# Computational Solid State Physics, part II

- **Instructor:** Lilia Boeri
- **Email:** [lilia.boeri@uniroma1.it](mailto:lilia.boeri@uniroma1.it)
- **Webpage:** <https://lboeri.wordpress.com>

# Outline: Solving K-S Equations in Practice

Kohn Sham Equation in Solids: Large Hilbert Space

Practical Problems:

- 1) Solving *Individual* Schroedinger's Equation Efficiently.

*solution*

- 2) Integrating the Individual Schroedinger's Equation over k space.

Focus is on solutions implemented in quantum espresso (plane-waves and pseudopotentials, k-space integration methods).

# Kohn-Sham Equations:

Kohn-Sham quasi-particles have eigenfunctions and eigenergies satisfying the single-particle equations:

$$\left( -\frac{1}{2} \nabla^2 + v_{ext}(\mathbf{r}) + \int \frac{n(\mathbf{r}')}{|\mathbf{r} - \mathbf{r}'|} d\mathbf{r}' + v_{xc}[n(\mathbf{r})] \right) \phi_i(\mathbf{r}) = \epsilon_i \phi_i(\mathbf{r})$$

With the **self-consistency** condition:

$$n_0(\mathbf{r}) = \sum_i |\phi_i(\mathbf{r})|^2$$

The **Total Energy** is given by:

$$E = 2 \sum_{j=1}^{N/2} \epsilon_j + E_{xc}[n(\mathbf{r})] - \frac{e^2}{2} \iint \frac{n(\mathbf{r}) n(\mathbf{r}')}{|\mathbf{r} - \mathbf{r}'|} d\mathbf{r} d\mathbf{r}' - \int d\mathbf{r} v_{xc}(\mathbf{r}) n(\mathbf{r})$$

# Kohn-Sham Equations for solids:

Since the Hamiltonian is lattice periodic, Kohn-Sham equations for a solid are diagonal in  $\mathbf{k}$  space:

$$v_{ext}(\mathbf{r}) = v_{ext}(\mathbf{r} + \mathbf{R}) \Rightarrow i = (n, \mathbf{k})$$

Hence Kohn-Sham self-consistent equations read:

$$\left[ -\frac{1}{2m_e} \nabla^2 + v_{ext}(\mathbf{r}) + v_H(\mathbf{r}) + v_{xc}(\mathbf{r}) \right] \phi_{n,\mathbf{k}}(\mathbf{r}) = \varepsilon_{n,\mathbf{k}} \phi_{n,\mathbf{k}}(\mathbf{r})$$

$$n(\mathbf{r}) = \sum_{occ} |\phi_{n,\mathbf{k}}(\mathbf{r})|^2$$

The **sum** over occupied states is a **sum over occupied bands**; this requires specialized methods.

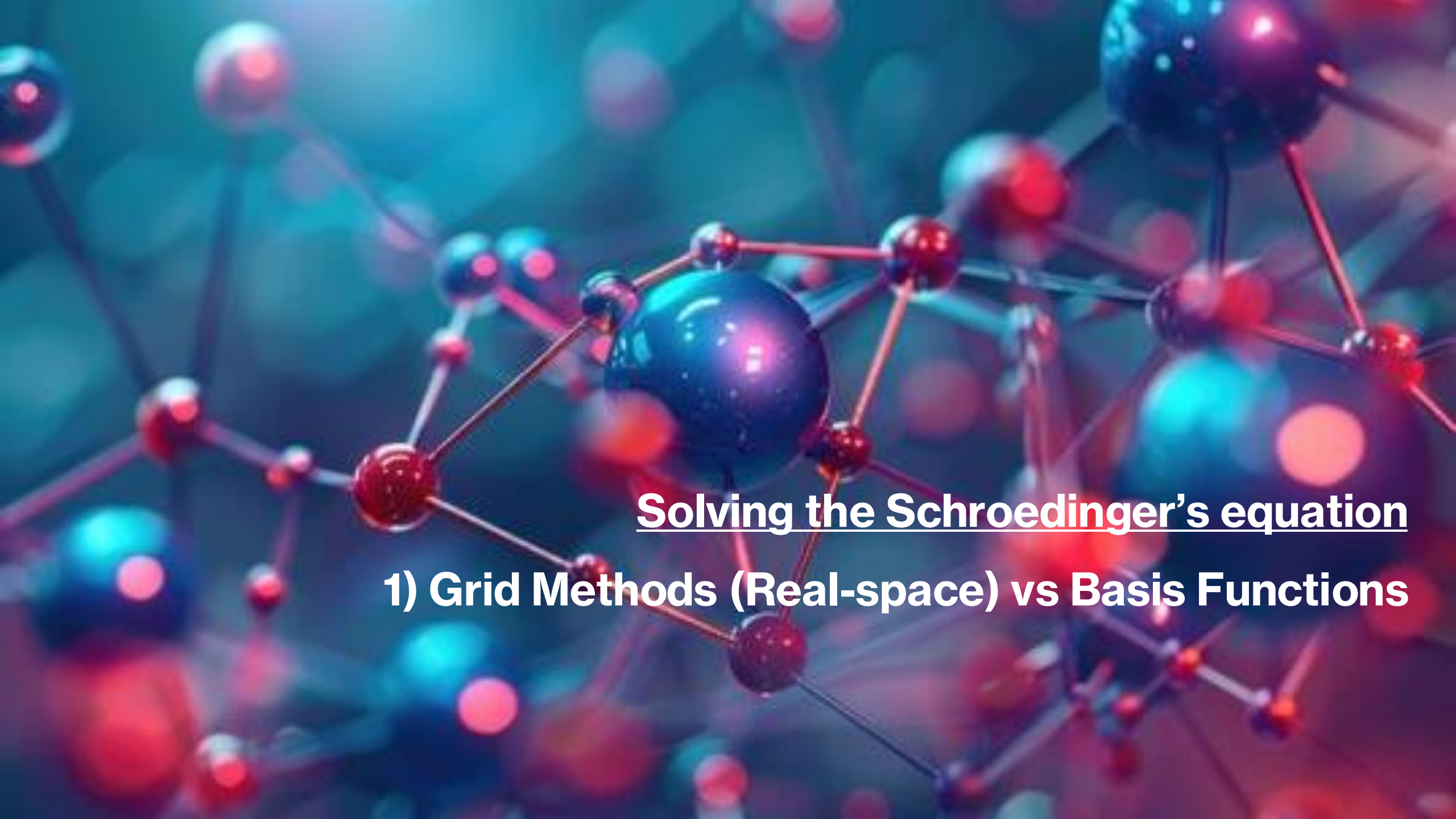
# Kohn-Sham Equations for solids:

$$v_{ext}(\mathbf{r}) = v_{ext}(\mathbf{r} + \mathbf{R}) \Rightarrow i = (n, \mathbf{k})$$

**Main Challenge:** Solve a **large number** ( $n, k$ ) of decoupled single-particle Schroedinger's equations (2° order differential equations) coupled through self-consistency condition.

► This requires:

- 1) Efficient methods to **solve the Schroedinger's equation** (grid vs basis functions).
- 2) Efficient methods to perform **k-space integration** (Use of symmetries, integration methods).



**Solving the Schroedinger's equation**

**1) Grid Methods (Real-space) vs Basis Functions**

# Solving the Schroediger's equation: Grid Methods

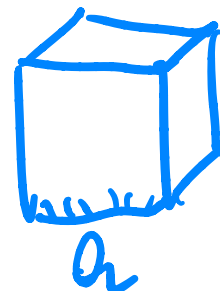
Kohn-Sham equations are 2° order differential equations:

$$\hat{T} \left( -\frac{1}{2} \nabla^2 + v_{ext}(\mathbf{r}) + \int \frac{n(\mathbf{r}')}{|\mathbf{r} - \mathbf{r}'|} d\mathbf{r}' + v_{xc}[n(\mathbf{r})] \right) \phi_i(\mathbf{r}) = \epsilon_i \phi_i(\mathbf{r})$$

The most straightforward way is to partition real-space in a **uniform mesh** of  $N_p^3$  points:

$$\mathbf{r} = \frac{a}{N_p} (p \mathbf{u}_x + q \mathbf{u}_y + r \mathbf{u}_z)$$

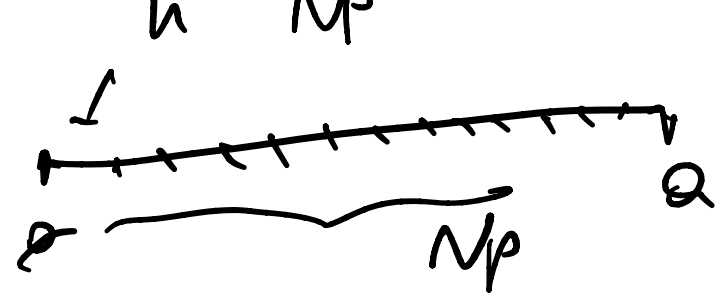
$$V_{k_s}(z)$$



Each K-S wavefunction is **discretized** into a set of  $N_p^3$  components:

$$\Phi(p, q, r) = \phi \left( \frac{p}{N_p} a \mathbf{u}_x + \frac{q}{N_p} a \mathbf{u}_y + \frac{r}{N_p} a \mathbf{u}_z \right)$$

$$h = \frac{a}{N_p}$$



# Solving the Schroediger's equation: Grid Methods

The **kinetic energy** is computed by **finite differences**:

$$\frac{\partial^2 \phi_i(r)}{\partial x^2} \simeq \left( \frac{N_p}{a} \right)^2 [ \Phi_i(p+1, q, r) - 2\Phi_i(p, q, r) + \Phi_i(p-1, q, r) ]$$

The **potential Energy** ( $V_{ks}(r)$ ) term is computed on the  $N_p^3$  grid giving:

$$V_{ks}(p, q, r)\Phi(p, q, r)$$



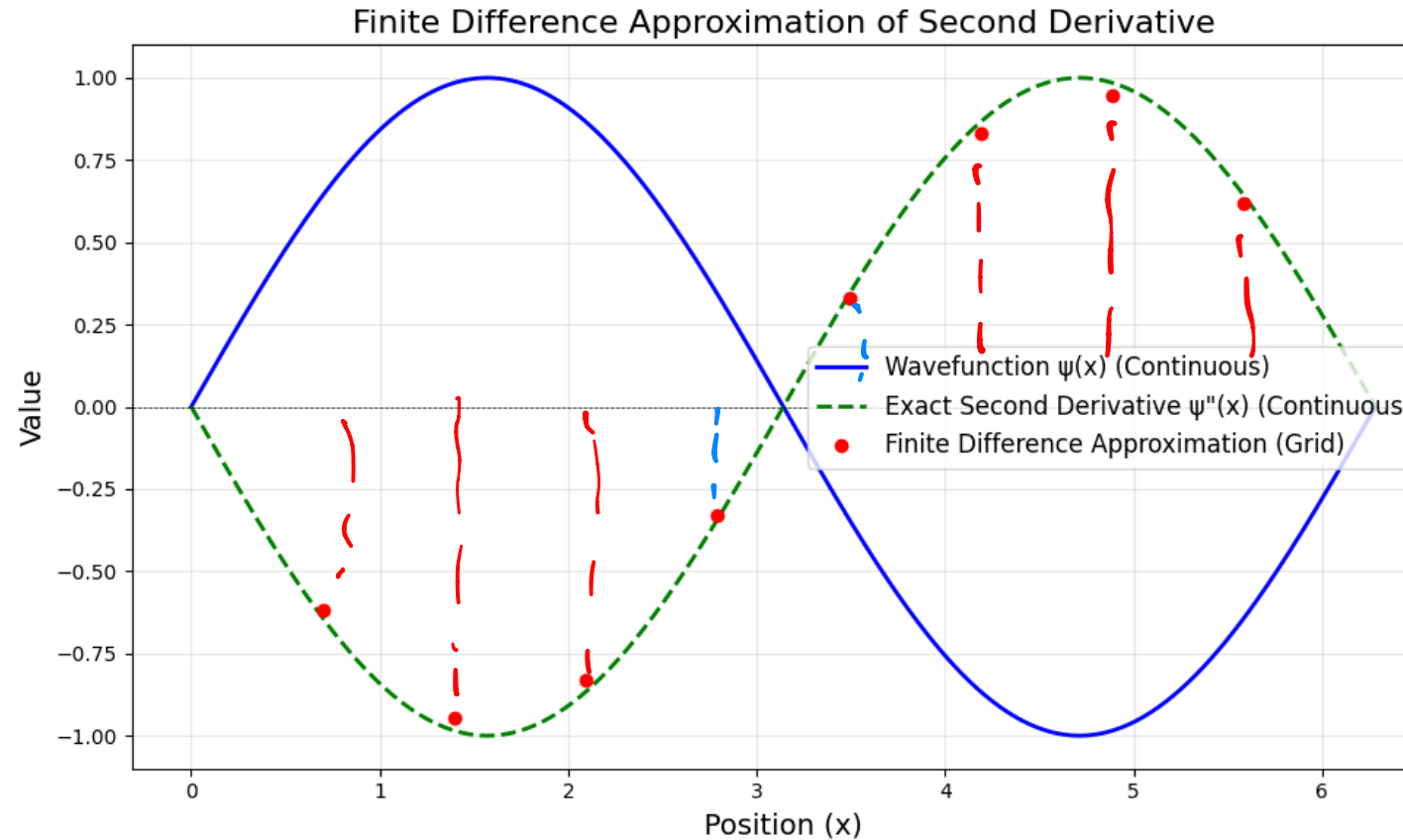
And **Periodic Boundary Conditions** are enforced by:

$$\begin{aligned}\Phi_i(N_p, q, r) &= \Phi_i(0, q, r) \\ \Phi_i(-1, q, r) &= \Phi_i(N_p - 1, q, r)\end{aligned}$$

## Second order derivative by Finite Differences:

$$\frac{\partial^2 \phi_i(r)}{\partial x^2} \simeq \left( \frac{N_p}{a} \right)^2 [ \Phi_i(p+1, q, r) - 2\Phi_i(p, q, r) + \Phi_i(p-1, q, r) ]$$

$$h = \frac{a}{N_p}$$



# Solving the Schroediger's equation: Grid Methods

Once all terms are written down, for each KS WF we have to diagonalize a  $N_p^3$  Sparse Matrix;

► 1d example ( $N_p \times N_p$  matrix):

Kinetic  
energy

$$H\phi_i = \epsilon_i\phi_i$$

$$h = \frac{a}{N_p}$$

$$H = \begin{bmatrix} V_1 - \frac{2}{h^2} & \frac{1}{h^2} & 0 & \cdots & 0 \\ \frac{1}{h^2} & V_2 - \frac{2}{h^2} & \frac{1}{h^2} & \cdots & 0 \\ 0 & \frac{1}{h^2} & V_3 - \frac{2}{h^2} & \cdots & 0 \\ \vdots & \vdots & \vdots & \ddots & \vdots \\ 0 & 0 & 0 & \frac{1}{h^2} & V_{N_p} - \frac{2}{h^2} \end{bmatrix}$$



p

$$\phi_i = \begin{bmatrix} \phi_i(0) \\ \phi_i(h) \\ \phi_i(2h) \\ \vdots \\ \phi_i(hp) \end{bmatrix}$$

p

↓

# Solving the Schroediger's equation: Grid Methods

## Scaling and Computational Costs:

- For a grid with resolution  $h$ , the error scales as:
- While the computational cost scales as:

$$\Delta = \mathcal{O}(h^2)$$

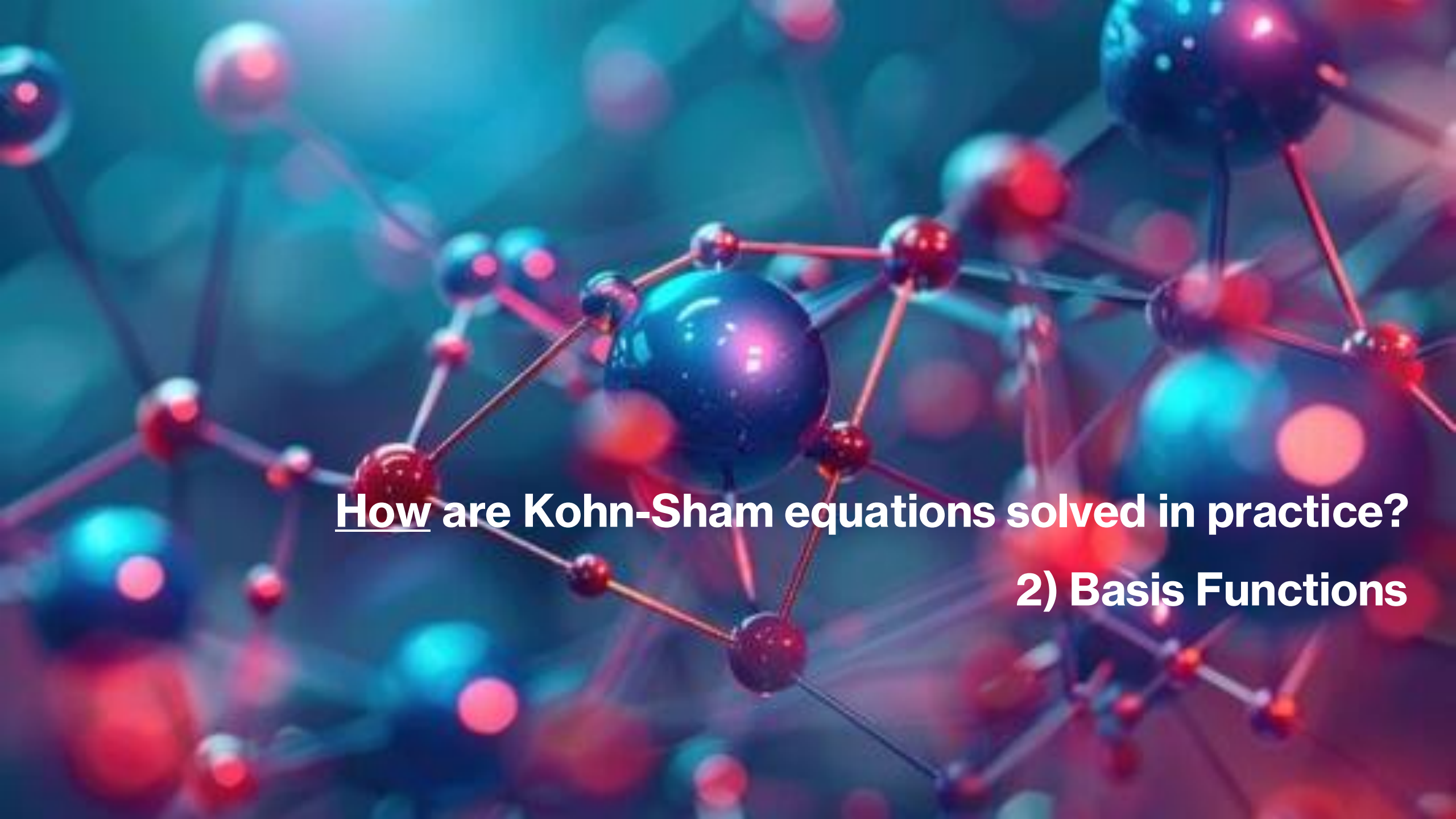
$$\text{Cost} = \mathcal{O}(h^{-d})$$

Independent  
on dimension  $d$

Grid methods become unpractical for  $d=3$ . For example, for a box of 20 Å, with resolution 0.1 Å, each K-S eigenfunction ( $i=n, k$ ) has  $\mathcal{O}(10^7)$  components!

# Famous Real-Space Codes:

- **Octopus**: <https://octopus-code.org/>
- **GPAW**: <https://wiki.fysik.dtu.dk/gpaw/>
- **PARSEC**: <https://parsec.ices.utexas.edu/>
- **BigDFT**: <https://bigdft.org/>
- **RSDFT**: <https://rsdft.riken.jp/>
- **NWChem**: <https://www.nwchem-sw.org/>
- **DFT-FE**: <https://github.com/dftfeDevelopers/dftfe>
- **RMG**: <http://www.rmgdft.org/>



# How are Kohn-Sham equations solved in practice?

## 2) Basis Functions

# Solving the Schroediger's equation: Basing Functions

Most modern codes for DFT do not solve K-S equations directly, but use an **expansion on basis functions** to transform a differential problem into a secular problem.

- 1) Expand Kohn-Sham orbitals  $\psi_j$  in an appropriate basis of known functions  $\{f_\alpha(\mathbf{r})\}$ :

$$\psi_j(\mathbf{r}) = \sum_{\alpha} c_{j\alpha} f_{\alpha}(\mathbf{r})$$

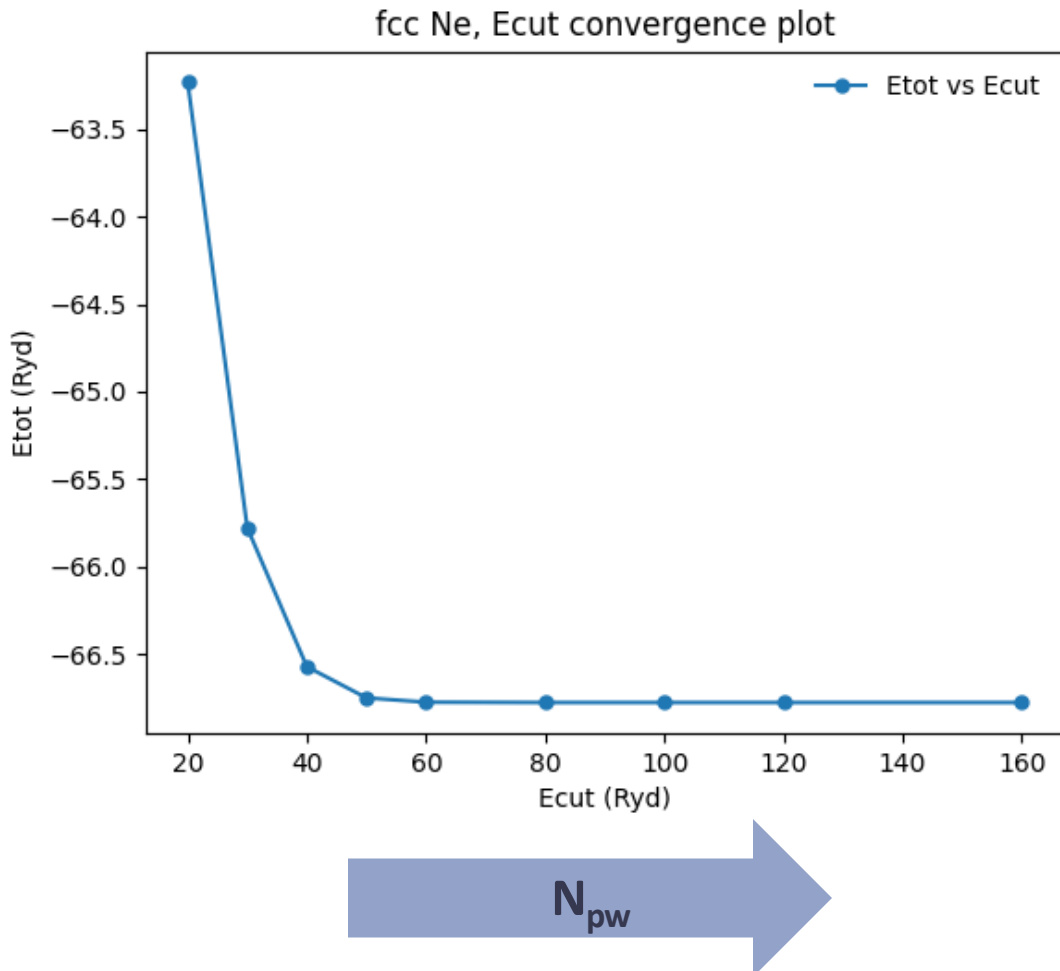
- 2) Left-multiply K-S equation by  $f_{\beta}(\mathbf{r})$  gives:

$$\sum_{\alpha} H_{\beta\alpha} c_{j\alpha} = \varepsilon_j c_{j\beta} \quad j = 1, \dots, N$$

The problem of solving the KS equations is reduced to **diagonalizing the matrix  $H_{\alpha\beta}$** .

The **Dimension** of the Hamiltonian matrix is determined by the **number of basis functions**.

**3) Variational Principle:** if the set of **basis** functions is **complete**, the total energy converges to the exact value from above (truncation of basis set).



**Example:** Total energy of fcc Neon, plane wave basis set.

# Most Common Types of Basis Functions:

## «Pure» Basis sets:

- **Localized Basis Functions: Gaussians, Slater-type orbitals, Muffin-Tin Orbitals** (Quantum Chemistry).
- **Delocalized Basis Functions: Plane Waves** (Periodic Solids).

## «Mixed» Basis sets:

*All-electron calculation*

- Based on a «smart decomposition» of solids into «atomic» and a delocalized (valence) region.  
**Example**, Linearly Augmented Plane Waves (LAPW), Linear Muffin Tin Orbitals – O. K. Andersen, Phys. Rev. B 12, 3060 (1975).

Quantum Espresso employs plane waves, which are a natural choice for solids.

# Grid Methods:

## Pros:

### Arbitrary Boundary Conditions:

- Handles periodic, non-periodic, or mixed systems easily.
- Suitable for molecules, clusters, surfaces, and isolated systems.

### 1. High Spatial Resolution:

- Accurately represents localized features, such as electron densities near nuclei.
- Adaptive mesh refinement (AMR) improves efficiency in key regions.

### Simplified Parallelization:

- Real-space grids are easily distributed across processors, scaling well on modern architectures.

### Time-Dependent Applications:

- Effective for real-time simulations and time-dependent density functional theory (TDDFT).

## Cons:

### High Memory and Computational Costs:

- Dense grids require significant memory and computational effort.
- Comp. cost increases quickly with system size.

### Handling Boundaries:

Careful implementation is required to apply correct boundary conditions.

### Symmetry Limitations:

Does not naturally exploit crystalline symmetries, making calculations less efficient for periodic systems.

### Numerical Challenges:

Finite-difference approximations can lead to numerical errors.

Requires careful grid spacing to balance accuracy and cost.

### Difficulty with High-Energy States:

Requires very fine grids to accurately represent oscillatory wavefunctions of high-energy states.

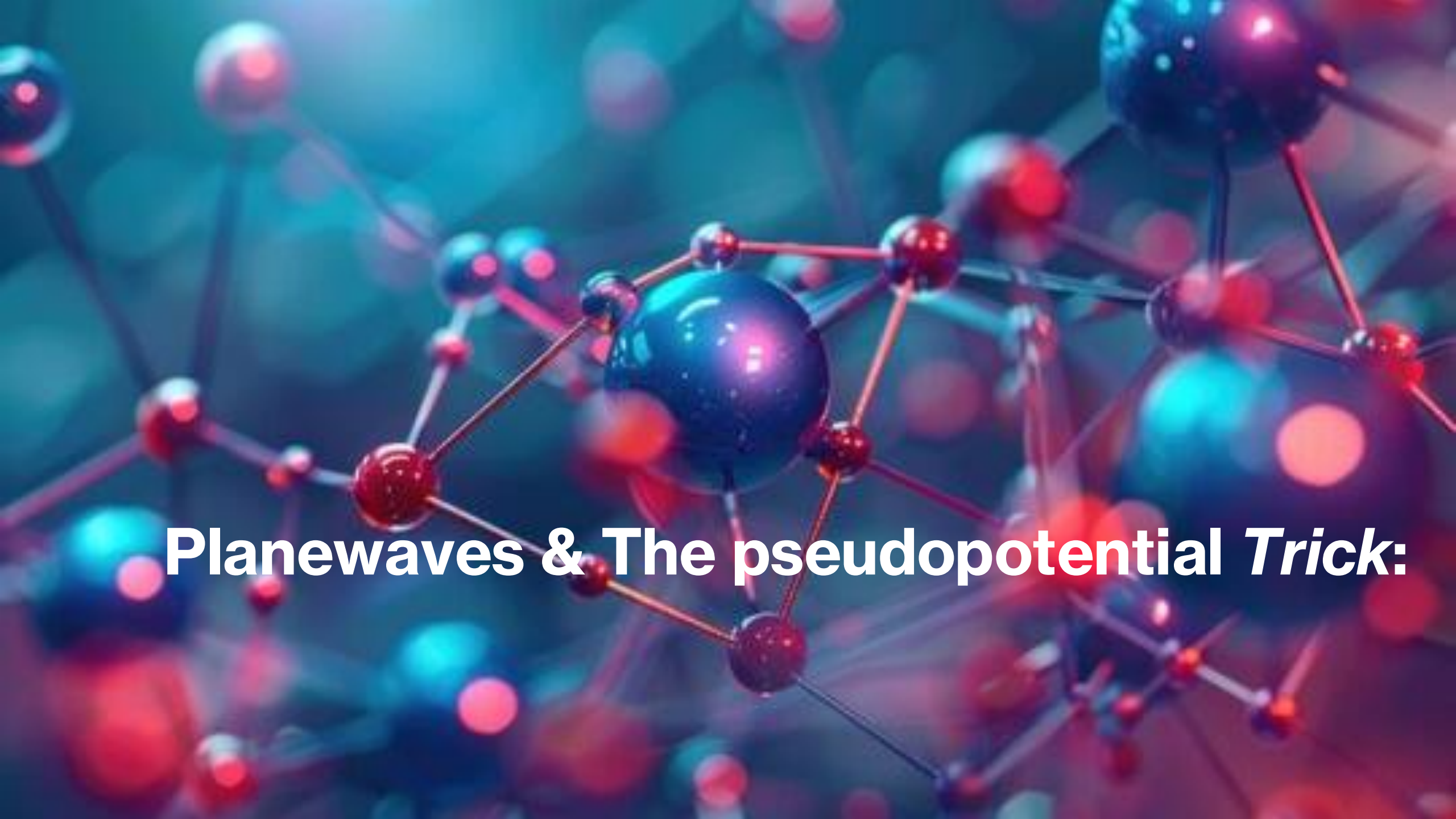
# Basis Functions vs Grid Methods:

## Pros:

- 1. Efficiency:** Require fewer parameters and smaller matrices, reducing computational cost.
- 2. Flexibility:** Adaptable for both localized (e.g., molecules) and periodic systems (e.g., crystals).
- 3. Periodic Boundary Conditions:** Naturally handled by plane wave basis sets.
- 4. Atomic Orbital Representation:** Localized basis sets resemble atomic orbitals, providing intuitive results.
- 5. Efficient Hybrid Functional Support:** Simplifies non-local exchange integral computations.

## Cons:

- 1. Basis Set Incompleteness:** Requires systematic tests for convergence.
- 2. Non-Orthogonality:** Can cause numerical instabilities in localized basis sets (e.g., Gaussian orbitals).
- 3. Core Features:** May need pseudopotentials to represent rapid oscillations near nuclei.
- 4. Specialization:** Requires choosing the right basis set for specific system types.



**Planewaves & The pseudopotential Trick:**

# Basis Functions: Plane Waves

Plane waves are a natural choice for periodic solids; They form a **complete, orthonormal basis set** (-> variational principle).

$$\langle \mathbf{r} | \mathbf{k} + \mathbf{G} \rangle = \frac{1}{V} e^{i\mathbf{k} + \mathbf{G} \cdot \mathbf{r}}, \quad \langle \mathbf{k} + \mathbf{G} | \mathbf{k} + \mathbf{G}' \rangle = \delta_{\mathbf{G}, \mathbf{G}'}$$

Kohn-Sham orbitals can be expanded as:

$$\phi_{n\mathbf{k}}(\mathbf{r}) = \frac{1}{\sqrt{\Omega}} \sum_{\mathbf{G}} c_{n\mathbf{k}}(\mathbf{G}) e^{i(\mathbf{k} + \mathbf{G}) \cdot \mathbf{r}} = \sum_{\mathbf{G}} c_{n\mathbf{k}}(\mathbf{G}) | \mathbf{k} + \mathbf{G} \rangle$$

$$c_{n\mathbf{k}}(\mathbf{G}) = \frac{1}{\sqrt{\Omega}} \int_{\text{cell}} \phi_{n\mathbf{k}}(\mathbf{r}) e^{-i\mathbf{G} \cdot \mathbf{r}} d\mathbf{r}$$

# Kohn-Sham Equations in plane waves:

Substituting the K-S orbital expansion into **Kohn-Sham Equations** we obtain the **secular equation**:

$$\sum_{\mathbf{G}'} [H_{\mathbf{G}, \mathbf{G}'}(\mathbf{k}) - \varepsilon_{n, \mathbf{k}} \delta_{\mathbf{G}, \mathbf{G}'}] c_{n, \mathbf{k} + \mathbf{G}'} = 0$$

$$H_{\mathbf{G}, \mathbf{G}'}(\mathbf{k}) = \frac{|\mathbf{k} + \mathbf{G}|^2}{2} \delta_{\mathbf{G}, \mathbf{G}'} + v_{\mathbf{G} - \mathbf{G}'}^{eff}$$

The potential term couples **G** and **G'**; For each  $n, \mathbf{k}$  we have to diagonalize a matrix with size  $\mathbf{N}_{pw} \times \mathbf{N}_{pw}$ .

# The pseudopotential trick:

The potential term couples  $\mathbf{G}, \mathbf{G}'$ ; For each value of  $k$  we have to diagonalize a matrix with size  $N_{pw} \times N_{pw}$ :  
**how can we keep the problem manageable?**

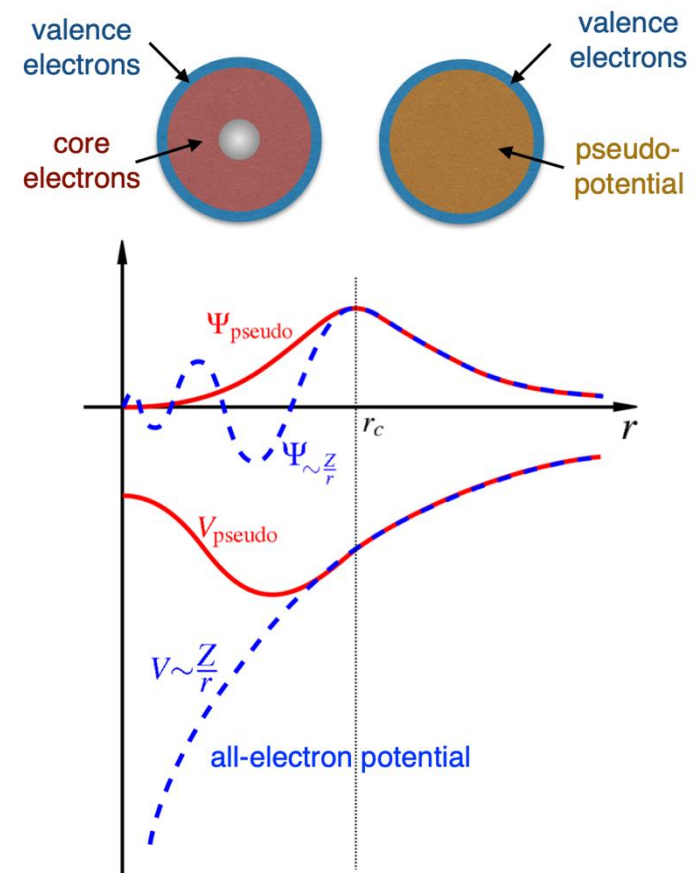
High- $\mathbf{G}$  components required to describe electrons in the **core** region →  
large  $N_{pw}$ .



Replace the all-electron potential with **pseudopotentials** taking into account core electron screening.

Core electrons are treated as chemically inert (frozen) → KS equations are solved for valence electrons.

There are different kinds of pseudos (Norm-conserving, ultrasoft, PAW...).



# How are pseudopotentials obtained in practice?

1. Solve the **all-electron** Schrödinger equation for the isolated atom.
2. Split electrons into **core** and **valence** (**frozen-core approximation**).
3. Construct **nodeless, norm-conserving** pseudo–valence wavefunctions that match the all-electron valence wavefunctions outside a chosen core radius.
4. Invert the radial Schrödinger equation to obtain the **atomic pseudopotential** corresponding to these pseudo–valence states.
5. **Unscreen** the pseudopotential by removing the valence Hartree and XC contributions of the atomic configuration, so that screening is rebuilt self-consistently in the solid and the pseudopotential remains transferable.

# 1) All-electron solution:

- For a **radially-symmetric** potential, the wavefunctions of an isolated **atom** can be **factorized** as:

$$\psi_{n\ell m}(\mathbf{r}) = R_{n\ell}(r) Y_\ell^m(\theta, \phi), \quad \ell = 0, \dots, n-1, \quad m = -\ell, \dots, \ell.$$

The radial part is solution of the equation:

$$\left[ -\frac{1}{2} \frac{d^2}{dr^2} + \frac{l(l+1)}{2r^2} - \frac{Z}{r} + v_H [n_c + n_v] + v_{xc} [n_c + n_v] \right] \chi_{nl}(r) = \varepsilon_{nl} \chi_{nl}(r)$$

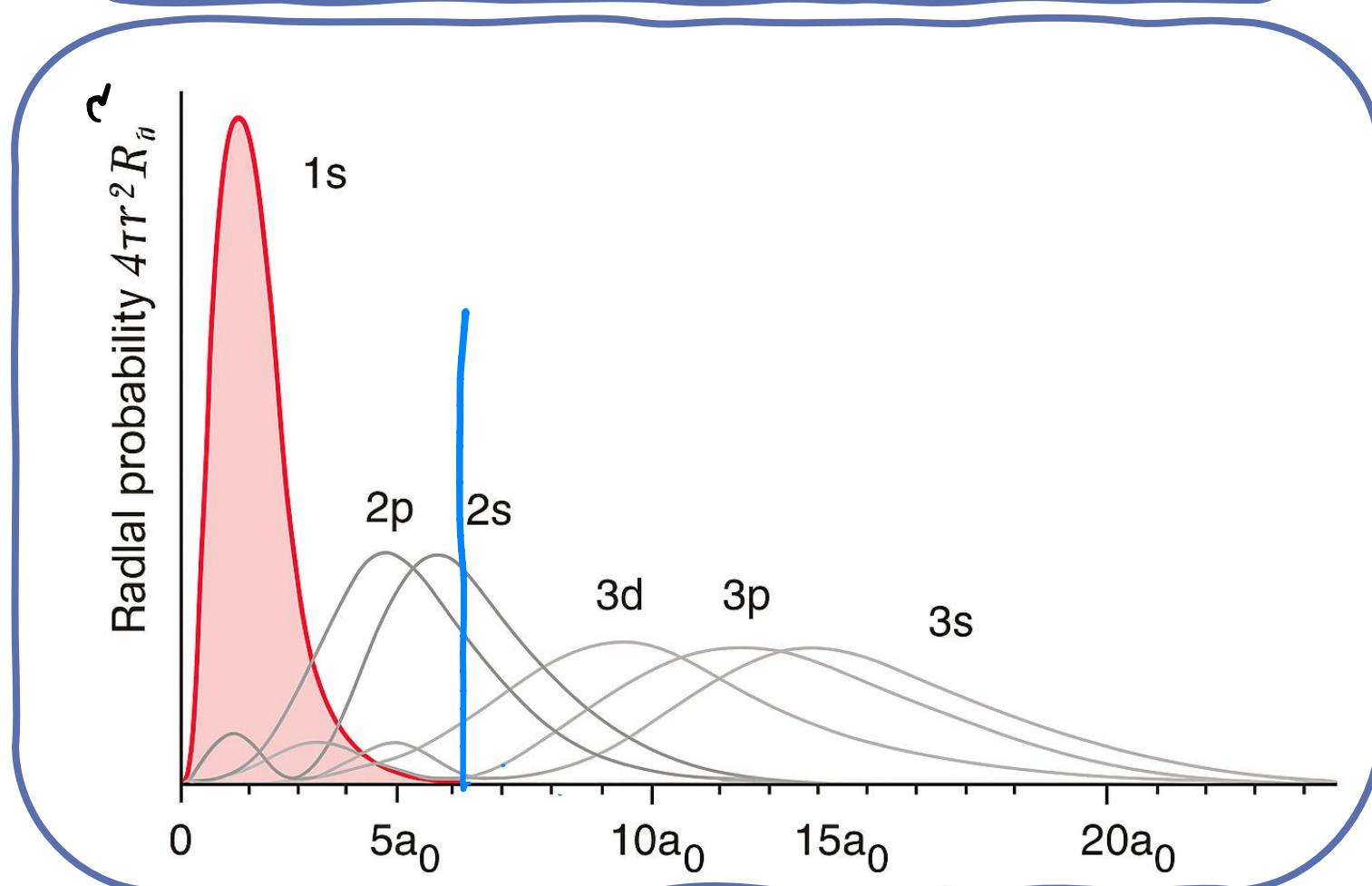
Where

$$\chi_{nl}(r) = r R_{n\ell}(r)$$

$$u_{n\ell}(r)$$

# 1) All-electron solution: hydrogenoid atom

$$R_{n\ell}(r) \propto \left(\frac{2Zr}{na_0}\right)^\ell e^{-Zr/(na_0)} L_{n-\ell-1}^{2\ell+1}\left(\frac{2Zr}{na_0}\right)$$



# 1) Frozen-core Approximation:

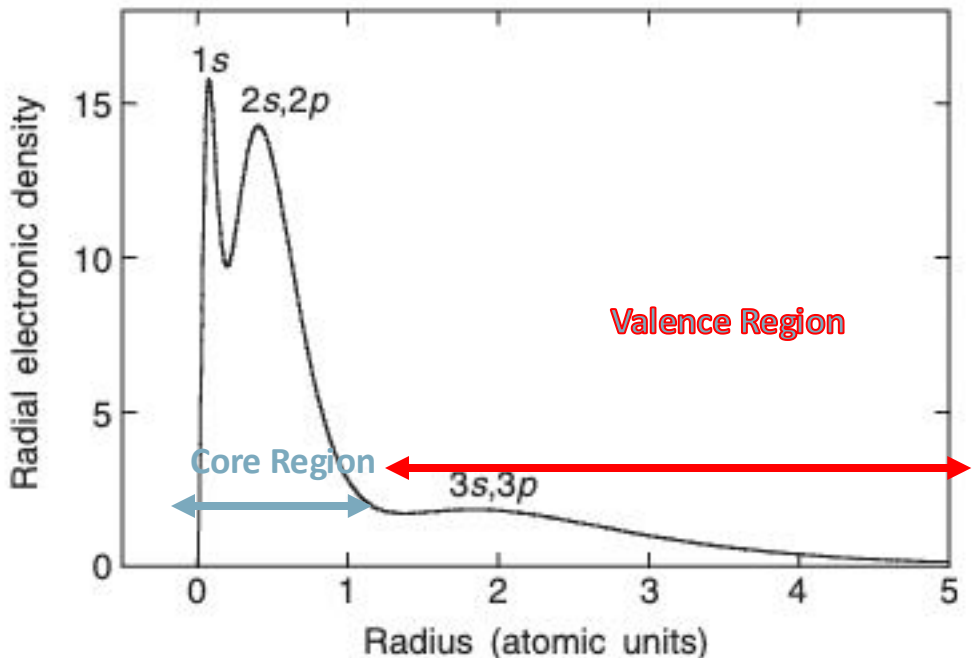
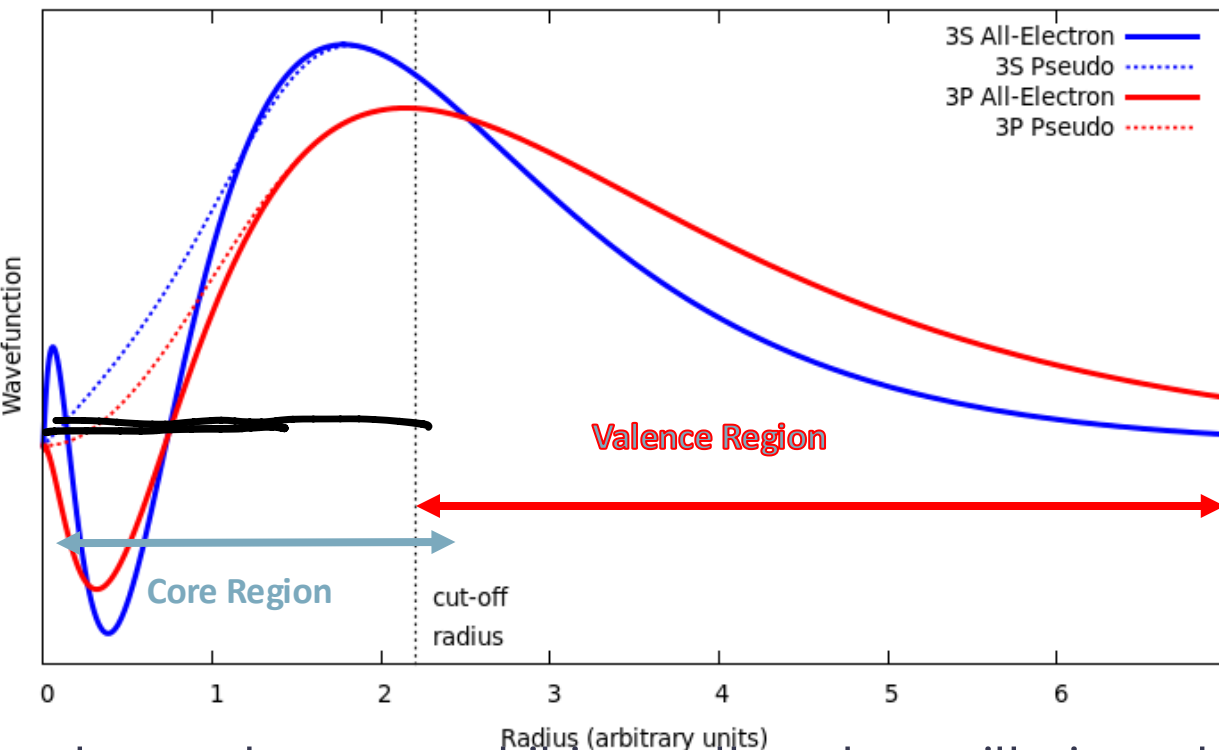


**Figure 1** Atomic shell structure: the example of silicon ( $Z = 14$ ). Top: the 14 ionization potentials of silicon, in electron volts (note the logarithmic scale). Bottom: radial electronic density as a function of the distance from the nucleus; both in energy (top) and in space (bottom), the core shells ( $1s$ ,  $n = 1$ , and  $2s$ ,  $2p$ ,  $n = 2$ ) are well separated from each other and from the valence  $3s$ ,  $3p$  shell ( $n = 3$ ).

Core and Valence charge exhibit very different localization in space: core charge «lives» close to the nucleus, **valence charge is «pushed» far away and determines chemical bonding.**

Pseudopotential idea: if the core is **inert**, it can be «dropped» (or **kept frozen**).

### 3) Construct Pseudo-Wavefunctions:



$$\chi_{n\ell}(r) = r R_{n\ell}(r)$$

- Close to the nucleus, valence electrons exhibit small-scale oscillations due to orthogonalization to the core states. These small-scale oscillations occur in the core region, and have no practical effect on bonding.
- The true (all-electron) wave function can be replaced by a pseudo-wavefunction without nodes (no small-scale oscillations), **which coincides with the original WF outside the core region (matching condition)**.

## 4) Invert Schroedinger's equation:

The pseudopotential is found **inverting the Schroedinger equation** for the pseudo-wavefunction, which has to obey the **matching conditions** with the corresponding all-electron wavefunction:

$$\left[ -\frac{1}{2} \frac{d^2}{dr^2} + \frac{l(l+1)}{2r^2} - \frac{Z}{r} + v_H^{full}(r) + v_{xc}^{full}(r) \right] \chi_{nl}(r) = \varepsilon_{nl} \chi_{nl}(r)$$

All-electron  
(full)

$$\left[ -\frac{1}{2} \frac{d^2}{dr^2} + \frac{l(l+1)}{2r^2} + \tilde{v}_{ps}^{nl}(r) \right] \chi_{nl}^{ps}(r) = \varepsilon_{nl} \chi_{nl}^{ps}(r)$$

Pseudo

$$\tilde{v}_{ps}^{nl}(r) = \varepsilon_{nl} + \frac{1}{2\chi_{nl}(r)} \frac{d^2\chi_{nl}(r)}{dr^2}$$

$$\tilde{v}_{ps}^{nl}(r) = v_{ps}^{bare}(r) + v_H[n_\nu] + v_{xc}[n_\nu]$$

However, the pseudopotential thus obtained includes the effect of e-e interaction. In order to make it fully transferable, it must be **unscreened**...

## 5) Unscreen the pseudopotential

Unscreening a pseudopotential removes the many-body screening effects of the valence electrons associated to the reference atomic configuration used to generate it:

All Electron (true atom):

$$\left[ -\frac{1}{2} \frac{d^2}{dr^2} + \frac{l(l+1)}{2r^2} - \frac{Z}{r} + v_H [n_c + n_v] + v_{xc} [n_c + n_v] \right] \chi_{nl}(r) = \varepsilon_{nl} \chi_{nl}(r)$$

Pseudopotential (only valence electrons):

$$\left[ -\frac{1}{2} \frac{d^2}{dr^2} + \frac{l(l+1)}{2r^2} + v_{screen}^{ps}(r) \right] \chi_{ps}(r) = \varepsilon_l \chi_{ps}(r)$$

$$v_{bare}^{ps}(r) = v_{screen}^{ps}(r) - v_H[n_v^{ps}] - v_{xc}[n_v^{ps}]$$

You download  
this?

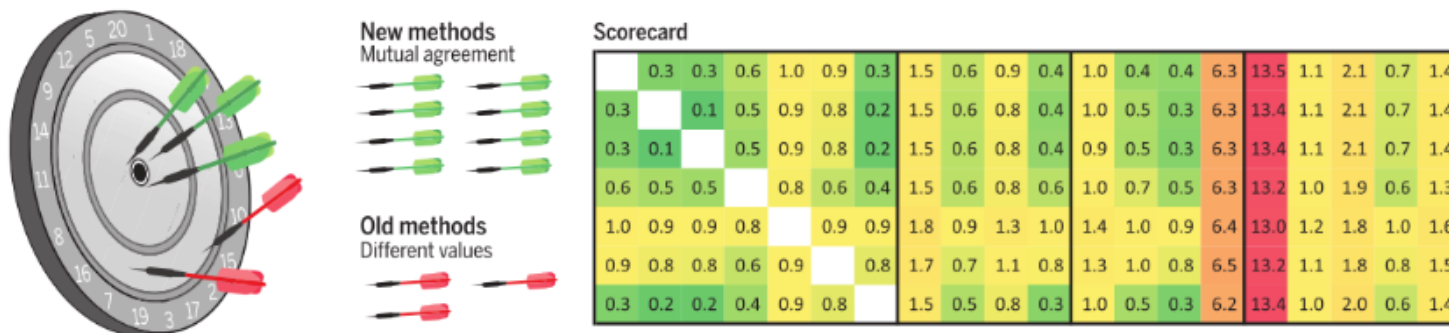
## Pseudopotential vs all-electron calculations

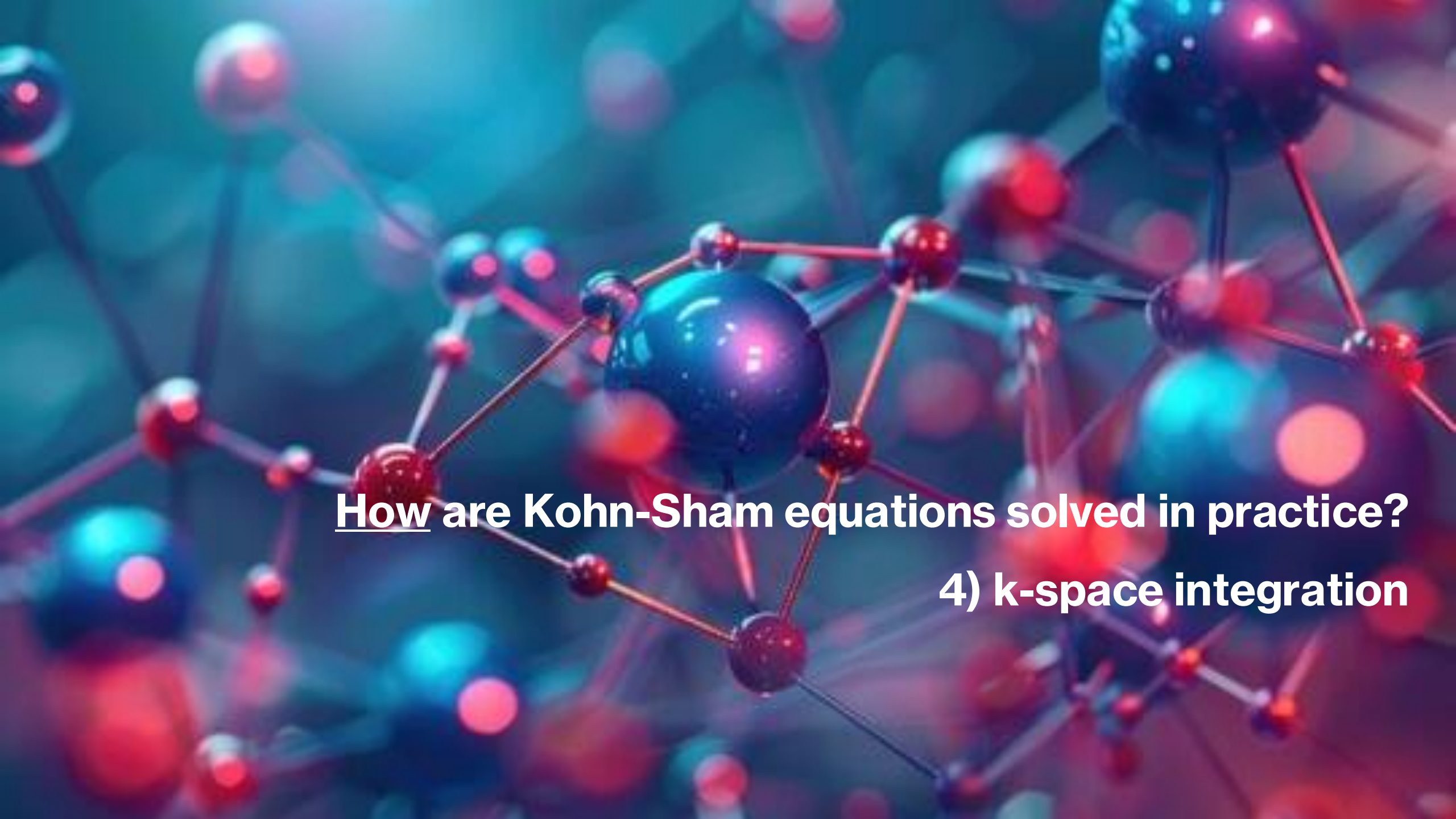
Systematic comparisons of different pseudopotential and all-electron DFT codes:  
*Reproducibility in density-functional theory calculations of solids*, K. Lejaeghere et  
al., Science 351 (6280), aad3000 (2016), DOI 10.1126/science.aad3000

Tests *precision* of the computational methods, not physical *accuracy* of results.

Main outcomes: 1) PPs and all-electron calculations have comparable precision, and  
2) everybody is converging towards the same set of results,

**Recent DFT methods yield reproducible results.** Whereas older DFT implementations predict different values (red darts), codes have now evolved to mutual agreement (green darts). The scoreboard illustrates the good pairwise agreement of four classes of DFT implementations (horizontal direction) with all-electron results (vertical direction). Each number reflects the average difference between the equations of state for a given pair of methods, with the green-to-red color scheme showing the range from the best to the poorest agreement.





How are Kohn-Sham equations solved in practice?

4) k-space integration

# Brillouin Zone Integration Methods:

The **integral** over **the Brillouin zone** is replaced by a **discrete sum** over a finite number of  $\mathbf{k}$  points, with **weights**:

$$\int_{\text{BZ}} f(\mathbf{k}) d\mathbf{k} \approx \sum_i w_i f(\mathbf{k}_i)$$

→ How to choose  $\mathbf{k}_i$ ,  $w_i$ ? Generate a **discrete mesh** of points in reciprocal space.

1. **Uniform Mesh** - *H. J. Monkhorst and J. D. Pack, Phys. Rev. B 13, 5188 (1976).*
2. **Special K points** - *A. Baldereschi, Phys. Rev. B 7, 5212 (1973); D. J. Chadi and M. L. Cohen, Phys. Rev. B 8, 5747 (1973).*
3. **Adaptive Meshes** (importance sampling).

# Generate a Discrete Mesh: *Uniform Grid*

*kpoints*

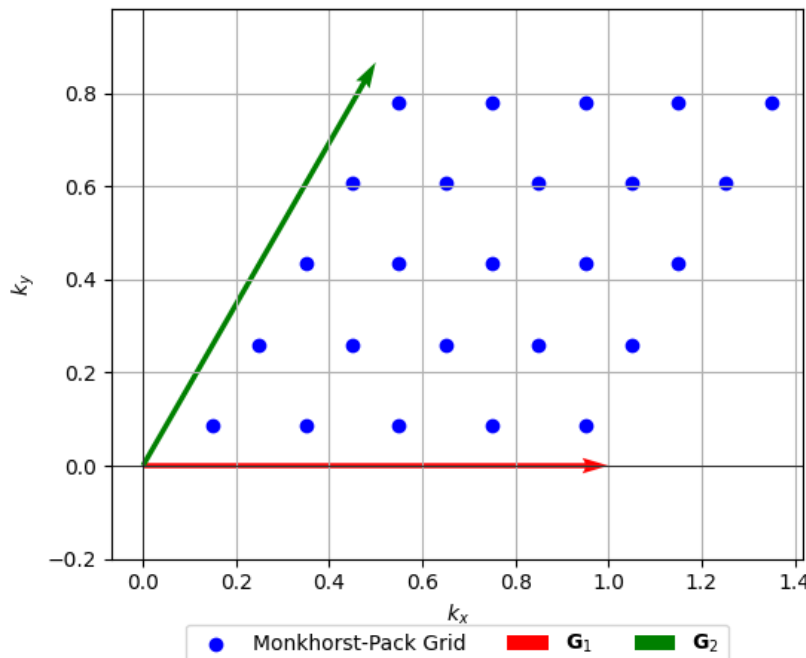
$n_1, n_2, n_3$

$$\mathbf{k_n} = \frac{n_1}{N_1} \mathbf{G}_1 + \frac{n_2}{N_2} \mathbf{G}_2 + \frac{n_3}{N_3} \mathbf{G}_3 + \mathbf{k}_{\text{shift}} \quad \text{with} \quad n_i = 0, 1, \dots, N_i - 1,$$

$\mathbf{G}_1, \mathbf{G}_2, \mathbf{G}_3$  : Reciprocal lattice vectors of the crystal,

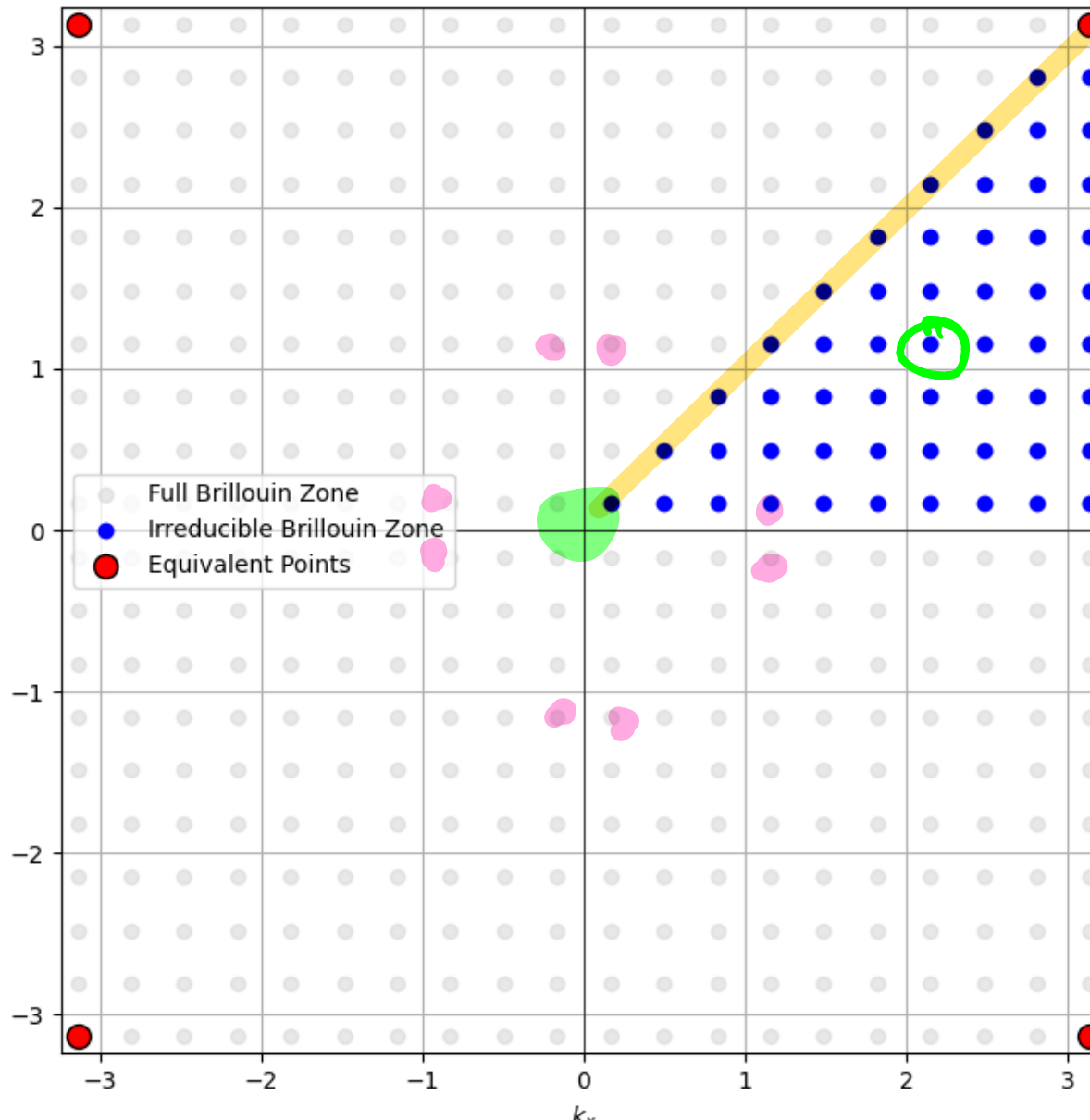
$N_1, N_2, N_3$  : Number of divisions along each reciprocal lattice direction,

$\mathbf{k}_{\text{shift}}$  : Optional shift applied to the k-point grid to avoid high-symmetry points.



H. J. Monkhorst and J. D. Pack, Phys. Rev. B 13, 5188 (1976).

# Use Symmetries to reduce to the Irreducible Wedge



# Use a k-space integration method:

Even after reducing to the Irreducible wedge, **the number of k points to achieve convergence** by brute-force summation is **too large**.

**K-space integration methods permit to reduce the sum to a manageable number of k points:**

- **Smearing Methods:** Delta functions are replaced by functions with a finite width (smearing).  
Different flavours of smearing functions: gaussians, «cold smearing» functions, etc.
- **Tetrahedron Method:** The Brillouin zone is partitioned into (small) tetrahedra; bands are calculated at the corners of the tetrahedra, and linearly interpolated inside.

# Smearing Methods:

Occupations, "smear"

**Delta functions** are replaced by functions with a finite width (**smearing**).

- Different **flavours** of smearing functions:

$$\delta(E - E_i) \approx \begin{cases} \frac{1}{\sqrt{2\pi}\sigma} \exp\left(-\frac{(E-E_i)^2}{2\sigma^2}\right), & \text{(Gaussian smearing)} \\ \frac{1}{\pi} \frac{\sigma}{(E-E_i)^2 + \sigma^2}, & \text{(Lorentzian smearing)} \\ \frac{1}{1+\exp\left(\frac{E-\mu}{k_B T}\right)}, & \text{(Fermi-Dirac smearing)} \end{cases}$$

**More advanced methods:** Methfessel-Paxton (Hermite Polynomials), cold smearing, etc...

## Tetrahedron Method:

*occupations "feheler"*

The Brillouin zone is partitioned into (small) tetrahedra; bands are calculated at the corners of the tetrahedra, and linearly interpolated inside.

$$\int_{BZ} f(\mathbf{k}) d\mathbf{k} \approx \sum_{\text{tetrahedra}} \int_{\text{tetrahedron}} f(\mathbf{k}) d\mathbf{k}.$$

$$f(\mathbf{k}) = \sum_{i=1}^4 w_i(\mathbf{k}) f_i,$$

where:

$w_i(\mathbf{k})$  are the barycentric weights, and  
 $f_i$  are the function values at the tetrahedron's four vertices.

# Tetrahedron Method:

$$\int_{BZ} f(\mathbf{k}) d\mathbf{k} \approx \sum_{\text{tetrahedra}} \int_{\text{tetrahedron}} f(\mathbf{k}) d\mathbf{k}.$$

- **Original Method:** O. Jepsen and O. K. Andersen, Solid State Comm., **20**, 1763 (1971);
- **Improved Tetrahedron Method (Metals):** P. E. Blöchl, O. Jepsen, and O. K. Andersen, Physical Review B **49**, 16223 (1994);
- **Improved Tetrahedron Method (Forces & Phonons):** Mitsuaki Kawamura, Yoshihiro Gohda, and Shinji Tsuneyuki, Phys. Rev. B **89**, 094515 (2014).

# Bonus: A short history of pseudopotentials

1. **Phillips-Kleinman Pseudopotentials (1959):** Projected out core states to simplify calculations by focusing on valence electrons. Phillips, J. C., & Kleinman, L.), *New method for calculating wave functions in crystals and molecules*. Physical Review, **116**(2), 287 (1959).
2. **Heine-Abarenkov Pseudopotentials (1964):** Empirical pseudopotentials designed for simple metals with free electron-like behavior. Heine, V., & Abarenkov, I. V. *On the derivation of a pseudopotential for a metal*. Philosophical Magazine, **9**(100), 451–465 (1964).
3. **Hamann-Schlüter-Chiang (HSC) Pseudopotentials (1979)** Norm conservation ensures accurate and transferable pseudopotentials. Hamann, D. R., Schlüter, M., & Chiang, C. *Norm-conserving pseudopotentials*, Physical Review Letters, **43**, 1494–1497 (1979).
4. **Bachelet-Hamann-Schlüter (BHS) Pseudopotentials (1982):** Tabulated HSC norm-conserving pseudopotentials for most elements. Bachelet, G. B., Hamann, D. R., & Schlüter, M. *Pseudopotentials that work: From H to Pu*, Physical Review B, **26**(8), 4199–4228 (1982).
5. **Vanderbilt Ultrasoft Pseudopotentials (USPP) (1990):** Relaxed the norm-conservation condition to improve computational efficiency and reduce basis set size. Vanderbilt, D. (1990), *Soft self-consistent pseudopotentials in a generalized eigenvalue formalism*, Physical Review B, **41**(11), 7892–7895 (1990).
6. **Troullier-Martins Pseudopotentials (1991):** Norm-conserving pseudopotentials optimized for smoothness and transferability. Troullier, N., & Martins, J. L. (1991), Efficient pseudopotentials for plane-wave calculations. Physical Review B, **43**(3), 1993–2006.
7. **Projector-Augmented Wave (PAW) Potentials (1994):** Combined pseudopotential techniques with all-electron accuracy for high efficiency and precision. Blöchl, P. E., *Projector augmented-wave method*, Physical Review B, **50**(24), 17953 (1994).
8. **ONCV Pseudopotentials (2013):** Optimized norm-conserving Vanderbilt pseudopotentials (accurate and efficient). Hamann, D. R., *Optimized norm-conserving Vanderbilt pseudopotentials*, Physical Review B, **88**(8), 085117 (2013).